

The Effects of Air Pollution on Health :

A Longitudinal Study of Los Angeles County Accounting for Measurement Error

Yanfei Qu, David A. Stephens

Abstract

This study develops a Bayesian hierarchical model to explore the effects of air pollution on respiratory and cardiovascular mortality in Los Angeles County. The model takes into account various pollutants such as $PM_{2.5}$, PM_{10} , CO, SO_2 , NO_2 and O_3 , as well as a related meteorological factor: temperature. The objective is to identify the significant factors affecting selected health outcomes without including all variables in each model specification. This flexibility enables the model to capture key drivers of health risk without redundancy. To account for potential measurement error in pollution data due to imperfect monitoring or averaging, certain observed pollutant levels are treated as noise proxies for true exposure. By specifying priors for regression coefficients and measurement error parameters and estimating posterior distributions via Markov Chain Monte Carlo (MCMC) sampling, it leads to more precise and reliable estimates of the health risks associated with air pollution exposure in Los Angeles County by incorporating both the count nature of the health data and the uncertainties in pollution measurements.

1 Introduction

Air pollution is one of the major global factors affecting public health, which leads to the public health disease most prominent in urban places as the concentrations of pollutants become augmented due to human activities and weather conditions [22]. Among pollutants, fine particulate matter (PM_{2.5}) and coarse particulate matter (PM₁₀) are especially alarming because they result in a wide range of adverse health outcomes. Since PM_{2.5} has a smaller size of particles, it can penetrate very deep in the respiratory system and circulatory system, leaving behind severe health consequences. Long-term and short-term exposure to PM_{2.5} has been linked to increased mortality risks from cardiovascular and respiratory diseases, as well as lung cancer [4][5]. Although PM₁₀ is less penetrating than PM_{2.5}, it causes serious health problems such as harming the respiratory system, aggravating asthma, and even inducing some chronic respiratory diseases [2]. Both PM_{2.5} and PM₁₀ are related to a systemic inflammatory and oxidative stress response that worsens hypoxic-induced conditions such as Chronic obstructive pulmonary disease (COPD) and heart disease. Short time exposure to PM_{2.5} and PM₁₀ shows acute impacts such as asthma attacks or even a heart attack, which may eventually lead to hospitalization for respiratory illness [17]. Moreover, studies have shown that PM₁₀ can act as a carrier for toxic substances such as heavy metals and organic compounds, further intensifying its health impacts [14] [8]. Other pollutants, including nitrogen dioxide (NO₂), sulfur dioxide (SO₂), carbon monoxide (CO), and ozone (O₃), compound these health burdens by triggering inflammatory responses and oxidative stress, associating with increased risk for adverse cardiopulmonary events [3]. For example, the association between NO₂ and pneumonia hospitalizations and asthma exacerbation rates is greater in children [23] while ozone build-up over hot days has been linked to respiratory distress and increased hospital admissions [7][1].

The development of modeling techniques allows for forecasting of pollution levels as well as the health impacts associated with it through simulation of dispersion and transformations of pollutants. Such methods would prove useful to investigate how any type

of emission changes in the atmosphere and how it makes changes to public health and the environment. Simultaneously, ongoing research tracks population health over time, supplying vital information that quantifies the cumulative impact of air pollution exposure. Yet much evidence exists for air pollution and health; intermediate effects for several weeks have not typically been studied. Using data categorized as weekly instead offers an avenue for smoothing out random spikes like those resulting from wildfires and revealing far higher trends while reducing variability due to transient conditions. Such medium-term analyses would thus help achieve that all-important balance between daily and long-term studies by giving a finer-resolution account of cumulative exposures and health impacts.

One pertinent issue in air pollution research is measurement error [18][6], which occurs due to the spatial misalignment between pollution monitors, population exposure, temporal variability of pollutants, and limitations in instruments used for monitoring. This error can obscure how estimates are and provoke bias, especially in terms of their intermediate applications. The most obvious example is that of fixed-site monitoring versus population-based exposure: fixed-site monitoring gives a point estimate that may not be aligned temporally with the individual subject's exposure. Correcting such measurement errors is indeed necessary for making findings valid; comprehensive and more advanced statistical methods, including hierarchical models, are required to address the uncertainty.

Los Angeles (L.A.) county poses for such research under high pollution levels from the combined effects of the vehicular emissions and geographic features creating temperature inversions trapping pollutants near the ground surface [16]. These conditions aggravate public health risks and warrant further localized assessment of health effects in that area. Temperature is also a central meteorological factor that influences how pollutants behave. Cold worsen respiratory diseases such as COPD, asthma, and pneumonia [19]. Cold vasoconstriction increases cardiovascular risks, while heat does so from dehydration and electrolyte imbalance, precipitating strokes and heart attacks. Air pollution has an additive effect in augmenting it, with climate-changing conditions bringing more

pollutants to concentration levels during warm months.

Advanced statistical modeling is critical for understanding the complex relationships between air pollution and health outcomes. Generalized linear models (GLMs) generally have been used for assessing associations, especially for counts, as in the case of mortality, hospital admissions, and other such cases, but they have linearity assumptions that may be too simple for the dynamics of exposure to pollutants [10]. Threshold effects or diminishing returns in the association between observers and pollutants are thus well identified by the use of general additive models (GAMs) which embed nonlinear smoothing functions [9][10]. Dynamic Linear Models (DLMs) further enhance temporal analysis by accounting for lagged effects, crucial for understanding delayed health impacts from pollutants like NO₂ and PM₁₀ [20][12]. While the ARIMA-GARCH models help handle trend and seasonality outcomes in modeling, in addition to accounting for fluctuations and autocorrelation in time series in drawing up volatility estimation specifically managing temporal patterns and volatility in pollution data [21][11]. Bayesian hierarchical models are particularly powerful for integrating spatial and temporal dependencies while addressing measurement error and multi-level variability, such as disparities in exposure across geographic regions or meteorological conditions [15][13]. These models enable the incorporation of prior knowledge, disentangling multi-pollutant effects, and accounting for uncertainties, thereby improving the robustness of the exposure-response relationship derived. Together, these advanced methodologies provide a comprehensive toolkit for exploring the intricate dynamics of air pollution and health impacts, ensuring accurate and actionable insights for public health and policy interventions.

This study uses a Bayesian hierarchical modelling framework with Poisson log-linear regression and AR(1) modelling to analyze the air pollution and health outcome weekly data for L.A. County. It incorporates temperature as a meteorological covariate, focusing on respiratory and cardiovascular health outcomes such as COPD, pneumonia, heart failure and malignant neoplasm, while addressing measurement errors. It requires the use of knowledgeable priors and uncertainty quantification to yield better approximation

estimates of health impacts over an intermediate time span. This research provides a clearer understanding of how a one-week lag in exposure to pollutants affects current health outcomes in the population of L.A. County. The ultimate goal is to improve public health awareness of the effects of air pollution and strategies that may be applied to areas at greatest risk, such as L.A.

The paper is organized as follows: Section 4 talks about the modeling framework. Section 4 provides a descriptive real data analysis and applies the models to real-world data interpreting health outcome effects. Finally, Section 4 renders the discussion against the previous work and puts forward future studies.

2 Analysis Methodology

Throughout, t indexes the time point, and the data consist of the observed death counts Y_t for the selected cause of mortality, P_t for the observed concentration of the selected air pollutant (the main variable of interest) of week t , T_t for the centered observed temperature of time t (i.e., this is obtained by subtracting the temperature mean from the observed temperature), C_t for the vector of observed covariates (data of other air pollutants) of week t , and offset_t for the offset term: in this case, the population size of week t . Here, $1 \leq t \leq N$, where $N=259$ is the number of weeks with valid measurements for all predictor and outcome variables within the selected time span: January 1st, 2018-December 17th, 2022.

Regarding the longitudinal process of the pollution data, we assume an underlying process X_t for the true log concentration of the observed main variable of interest: P_t . We propose a Poisson distribution for Y_t (i.e. the death counts due to a specific cause):

$$Y_t \sim \text{Poisson}(\lambda_t),$$

$$\log(\lambda_t) = \log(\text{offset}_t) + \beta_0 + \beta_1 T_{t-1} + \beta_2 X_{t-1} + \beta^\top \log(C_{t-1}),$$

where:

- β_0 is the intercept,
- β_1 quantifies the multiplicative effect of the lagged temperature T_{t-1} on Y_t ,
- β_2 represents the multiplicative effect of the log-transformed lagged true concentration of the selected air pollutant X_{t-1} on Y_t ,
- β is the coefficient vector capturing the multiplicative effects of the log-transformed lagged additional covariates C_{t-1} on Y_t .

The observed concentration of the selected air pollutant P_t is assumed to be measured with error relative to the logged true concentration X_t . The measurement error model is defined as:

$$\log(P_t) = X_t + \epsilon_x, \quad \epsilon_x \sim \mathcal{N}(0, \sigma_x^2/n_t),$$

where ϵ_x represents the measurement error, σ_x^2/n_t is the variance of the measurement error, and n_t is the number of valid daily measurements for air pollutant P within week t . Since the real data used in our subsequent analysis are collected from stations on a daily, every three days, or every six-day basis, and occasional reporting gaps occur due to malfunctions or other issues, this measurement error modeling structure, therefore, allows for more accurate observed data where larger n_t increases the precision of observed measurements by reducing the fluctuation of the measurement error. More discussion about the data will come in Section 4.

The true logged pollutant levels X_t are modeled as an autoregressive process of order 1 (AR(1)):

$$X_t = \mu + \phi(X_{t-1} - \mu) + \epsilon_{\text{AR}}, \quad \epsilon_{\text{AR}} \sim \mathcal{N}(0, \sigma_{\text{AR}}^2),$$

where μ is the overall mean of the pollutant process, ϕ is the autoregressive coefficient, and ϵ_{AR} is the process noise with variance σ_{AR}^2 , capturing random fluctuations over time.

A time-invariant-mean model is proposed for comparison with two other time-varying-

mean models in evaluating the AR(1) process of the underlying time series. The invariant-mean model assumes that $\mu_t = \mu$ is constant for all t . To better address the seasonal patterns, we extend this model to allow for a time-varying mean. One approach is to model μ_t as a simple harmonic function:

$$\mu_t = \alpha_0 \cos(2\pi\lambda(t + \omega)), \quad \lambda = \frac{1}{52}, \quad (1)$$

where α_0 captures the magnitude of the periodic effect, and ω accounts for the phase shift. To further capture the complexity of the seasonal patterns, we propose an alternative model for μ_t :

$$\mu_t = \alpha_0 g_1(2\pi\lambda(t + \omega), b_1, c_1) + \alpha_1 g_2(2\pi\lambda(t + \omega), b_2, c_2), \quad \lambda = \frac{1}{52}, \quad (2)$$

where

$$g_1(t, b, c) = \sqrt{\frac{1 + b^2}{1 + b^2 \cos^2(t)}} \cos(t + c \cos(t)),$$

$$g_2(t, b, c) = \sqrt{\frac{1 + b^2}{1 + b^2 \sin^2(t)}} \sin(t + c \sin(t)).$$

These models are designed to capture seasonal patterns in the pollution data, such as irregular consecutive peaks or sharp troughs. Their performance will be directly assessed by predictions on real-world air pollution data, as detailed in Section 4.

Simulation studies of the proposed outcome model and state space model are conducted in R using the packages `DLM`, `rjags`, and `rstan` to evaluate model robustness and determine the most suitable package for the final implementation in this study. The simulation results are presented in **Supplementary Material 4**.

3 Application to the Los Angeles County Data

A total of 11 air quality monitoring stations, accredited by the [U.S. Environmental Protection Agency \(EPA\)](#), have been established in Los Angeles County, California, USA, to

collect daily air pollution data. The daily data have been aggregated to create consistent time series aligned with the Morbidity and Mortality Weekly Report (MMWR) weeks¹ specific to this study. The locations of these monitoring stations are displayed in Figure 1.

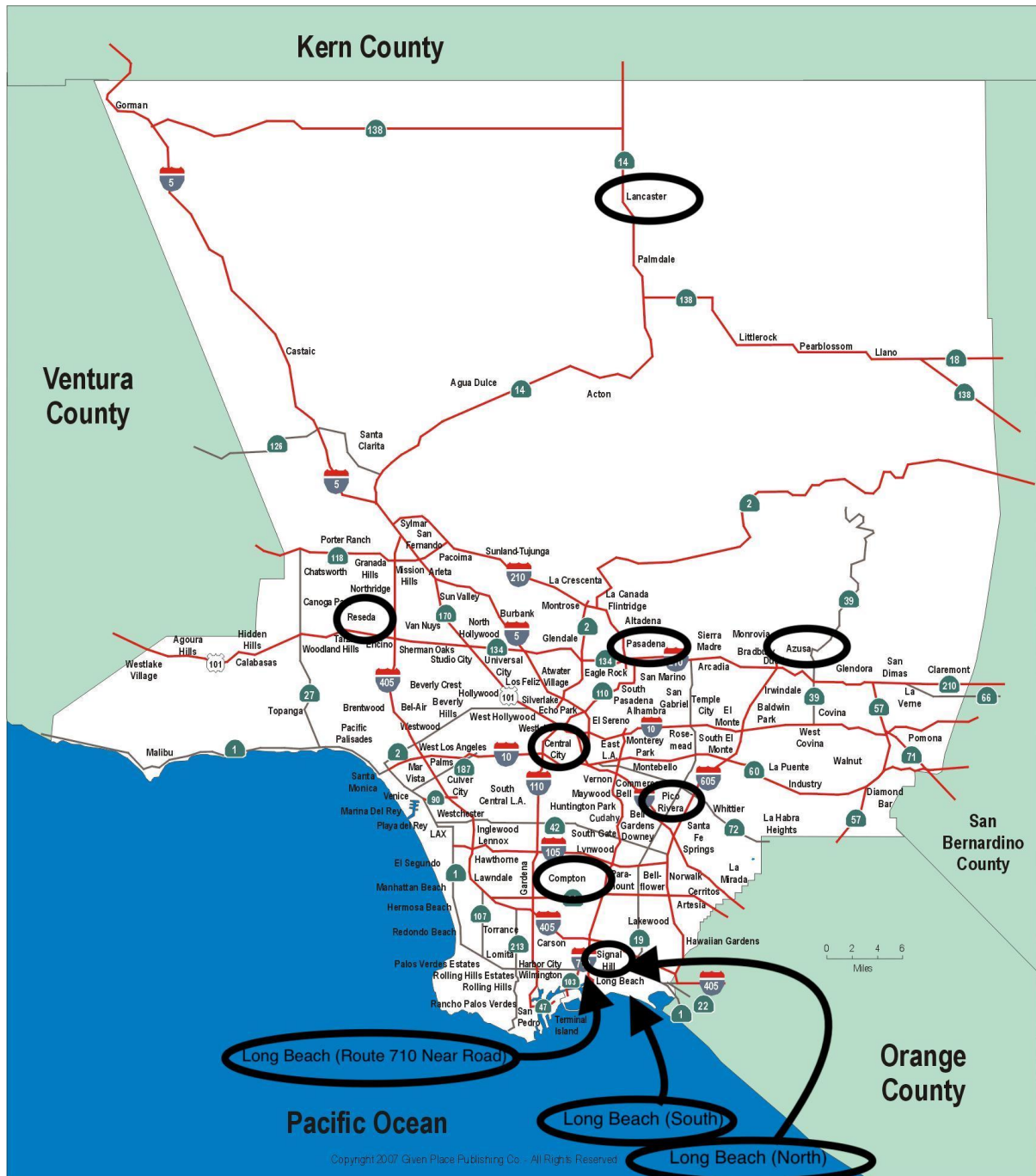


Figure 1: Locations of the EPA monitoring stations in L.A. County. Source: [maps Los Angeles](#)

¹MMWR weeks are defined as the periods from Sunday to Saturday, ranging from week 1 to week 52.

The daily temperature means for Los Angeles County are sourced from [NOAA's NClmGrid Daily Averages](#). MMWR weekly mean temperatures are calculated by averaging the corresponding MMWR daily means.

The population data for Los Angeles County is obtained from the [Federal Reserve Economic Data \(FRED\)](#) platform. Weekly population values are estimated from annual population data using simple linear regression.

The CDC WONDER platform provides access to health-related datasets, including weekly county-level counts of respiratory and cardiovascular deaths, along with temperature and quality data from January 1, 2018, to December 17, 2022. These datasets are available through the [About Provisional Mortality Statistics, 2018 through Last Week](#), with the source being the [Centers for Disease Control and Prevention \(CDC\)](#).

Detailed descriptions of the data sources and the aggregation process for the variables mentioned above are provided in **Supplementary Material 4**.

3.1 Descriptive data analysis

Table 1 summarizes the distribution of death counts, temperature, and air pollutant levels in L.A. County, from January 1st, 2018, to December 17th, 2022, covering a total of 259 MMWR weeks. Table 2 further presents the correlation matrix, which highlights the relationships between various air pollutants and temperature over the study period. Over the five-year span, the mean weekly concentrations of major air pollutants in L.A. County are as follows: PM_{2.5} at 11.57 $\mu\text{g}/\text{m}^3$, PM₁₀ at 26.45 $\mu\text{g}/\text{m}^3$, CO at 0.36 ppm, SO₂ at 0.36 ppb, NO₂ at 13.89 ppb, and O₃ at 0.03 ppm. Temperature (Figure 3), with a mean value of 17.28 °C, fluctuated between 4.95 °C and 30.14 °C. Time-series analyses reveal distinct seasonal patterns in the levels of these pollutants. Temperature was negatively related to CO and NO₂ concentrations (Figures 2c and 2d). These decreased during the warmer months, while O₃ (Figure 2f) almost mimicked the temperature trend, having severe concentrations during hot months. The trend of SO₂ (Figure 2e) levels reduced from

2018 to 2019, plateaued, then rose again after 2019. $PM_{2.5}$ and PM_{10} levels remained more or less the same but did show higher winter peaks during 2020-2021. Mortality over five years reached 40,982, of which 10,287 were due to COPD, 8,038 due to pneumonia, 11,541 due to neoplasms, and 11,116 due to heart failure. The average number of deaths reported weekly rose to 158, with higher peaks during colder months, thus confirming a relationship between temperature and mortality. Time series plots show random patterns for neoplasms (Figure 4c), while all other causes (Figures 4a, 4b, and 4d) exhibit seasonality with spikes at the beginning and end of the year.

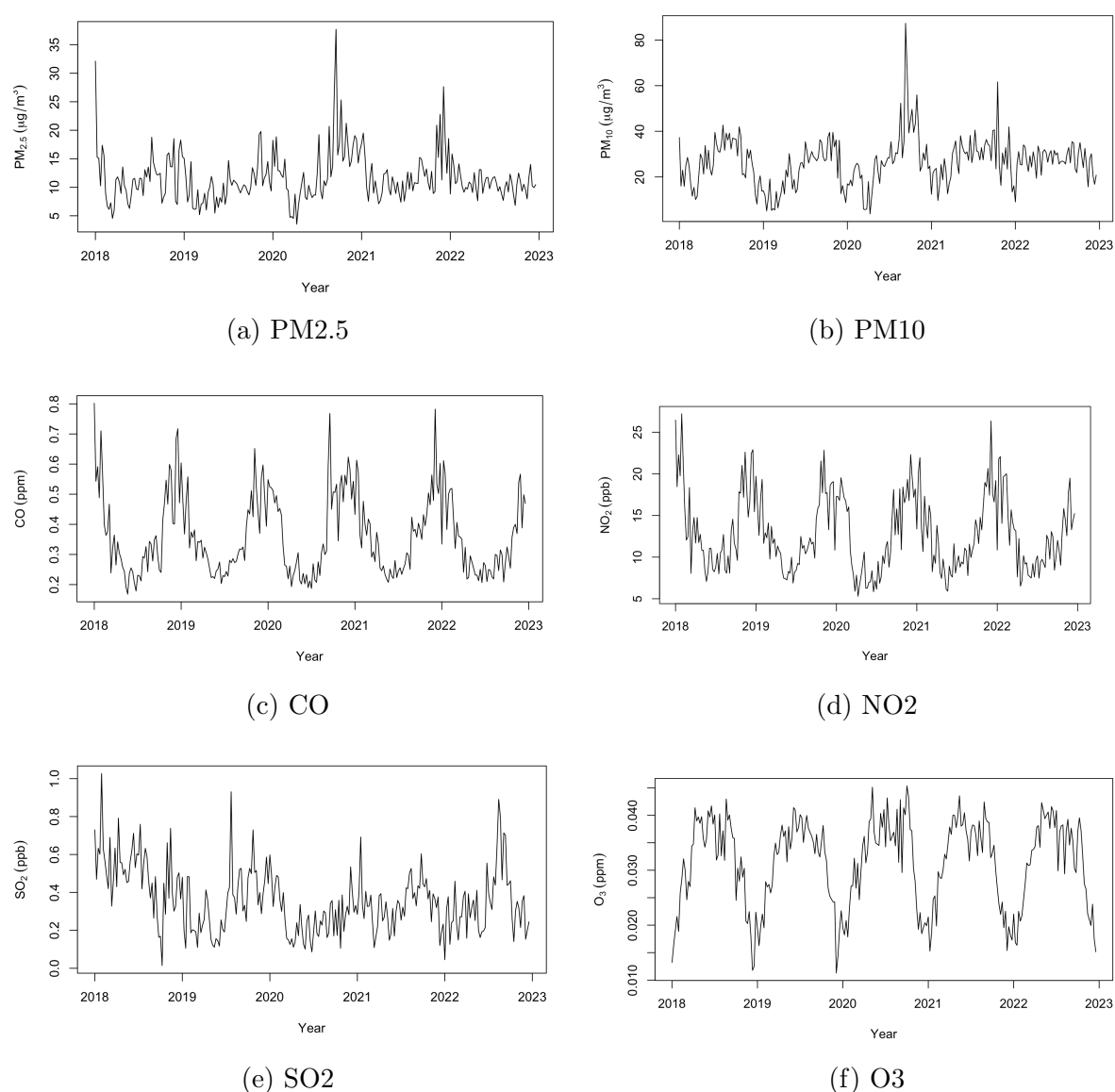


Figure 2: Time series of various air pollutants in L.A. county (January 1, 2018 - December 17, 2022)

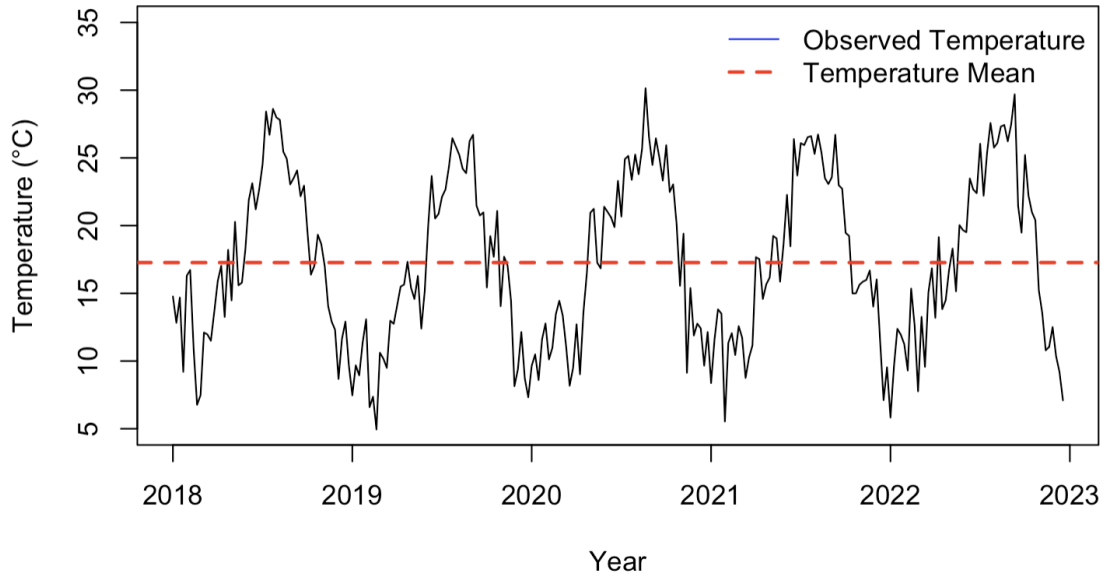


Figure 3: Temperature time series in L.A. county (January 1, 2018 - December 17, 2022)

3.2 Air pollution time series modelling

We use O_3 as an example and fit an AR(1) model to the log-scale deviations of O_3 , considering both the constant-mean structure and time-varying-mean structure (as described in Equations 1 and 2). Model comparison is made with the help of WAIC values, with superior performance being displayed by the invariant-mean model at 9,031,459,662 against 20,246,281,362 and 156,081,941,189 of the two types of time-varying-mean models, respectively. Additionally, by examining the plots comparing real log-scale deviations of O_3 vs. estimated log-scale deviations of O_3 (plots are provided in the **Supplementary Material 4**), it becomes evident that the invariant-mean model captures seasonal variations sufficiently. We, therefore, opt in using the invariant-mean AR(1) process log-scaled predictors outcome model.

The state space model with a constant mean for the AR(1) process is run in rjags for pollution data of all air pollutant types; parameters ϕ , σ_w^2 , and σ_v^2 are estimated through MCMC and DLM. The Appendix presents a summary in Table 4 for such estimates related to pollution measurement errors, considering a time-invariant mean in the AR(1) process.

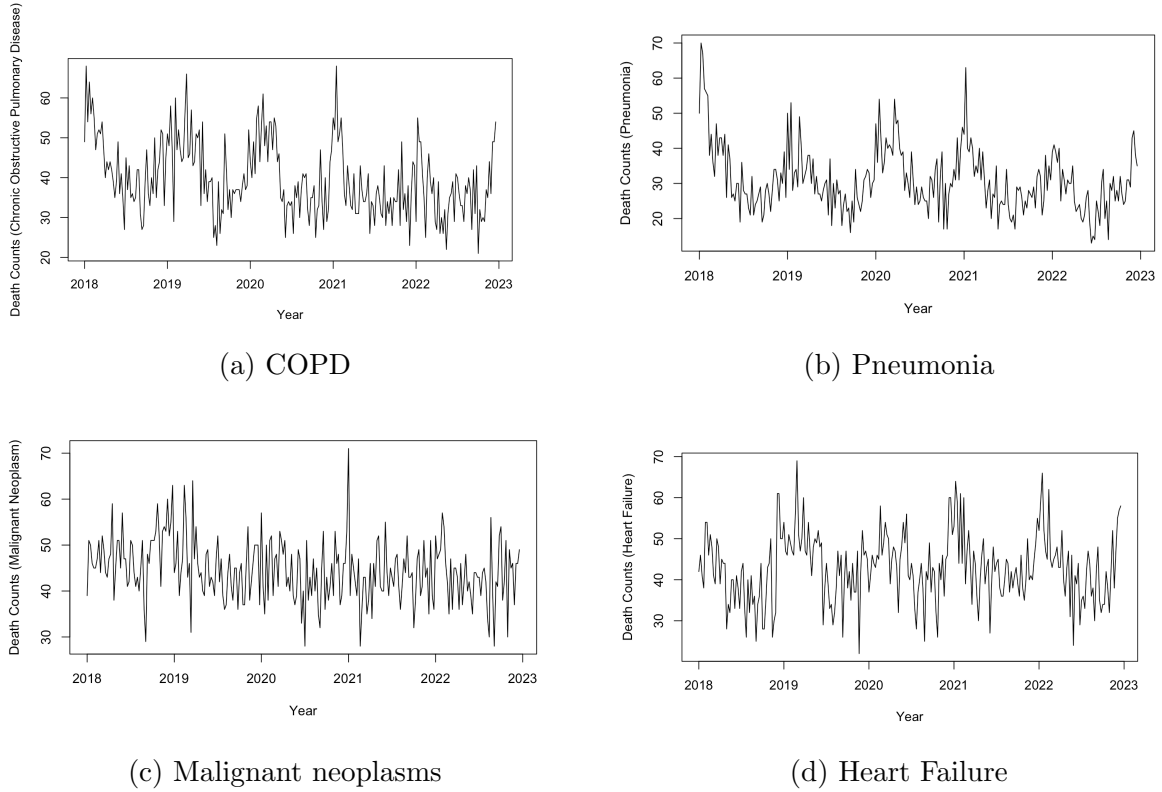


Figure 4: Time series of various health outcomes in L.A. County from January 1, 2018, to December 17, 2022.

The observed log-scaled predictors and their estimated true values on the log scale, from the AR(1) time-invariant-mean model, are reasonably similar, indicating that the Dynamic Linear Model (DLM) effectively captures the underlying relationships between the predictors and their true values. These plots are provided in [Supplementary Material 4](#).

3.3 Prior distributions in the Bayesian model

Based on the model framework detailed in Section 4, we place prior distributions on all unknown parameters in the Bayesian framework as follows: $\mu \sim \mathcal{N}(\mu_{P_t}, 0.1)$, where μ_{P_t} is the log mean of the observed level of the selected main air pollutant and 0.1 represents prior uncertainty; $\phi \sim \text{Uniform}(0, 1)$, reflecting expected exponential decay in the pollution autocorrelation function (ACF), ensuring positive autocorrelation and stationarity between consecutive measurements; The intercept (β_0) indicates the baseline mortality level, (β_1) reflects the temperature effects, (β_2) accounts for the selected pollutant impact;

		Mean	SD (σ)	Percentage				
				Min	25	Median	75	Max
Air pollutants concentration	PM _{2.5} ($\mu\text{g}/\text{m}^3$ ²)	11.57	4.15	3.54	8.99	10.83	13.20	37.69
	PM ₁₀ ($\mu\text{g}/\text{m}^3$)	26.45	10.42	3.79	20.58	26.69	31.66	87.34
	CO (ppm ³)	0.36	0.13	0.17	0.25	0.32	0.43	0.78
	SO ₂ (ppb ⁴)	0.36	0.17	0.01	0.24	0.34	0.46	1.03
	NO ₂ (ppb)	13.89	5.08	5.68	9.77	12.82	16.22	29.56
	O ₃ (ppm)	0.03	0.01	0.01	0.02	0.03	0.04	0.05
Temperature	Temperature ($^{\circ}\text{C}$)	17.28	6.13	4.95	12.32	16.61	22.66	30.14
Weekly deaths, count	COPD	40	9.23	21.00	33.00	38.00	45.75	68.00
	Pneumonia	31	9.11	13.00	25.00	30.00	35.75	70.00
	Neoplasm	45	6.72	28.00	40.00	45.00	49.00	71.00
	Heart Failure	43	8.32	22.00	38.00	43.00	47.00	69.00

Table 1: Summary statistics of weekly variables (January 1, 2018 - December 17, 2022). Note: "1 $\mu\text{g}/\text{m}^3$ " represents one microgram (10^{-6} grams) of pollutant per cubic meter of air; "ppm" is milligrams per liter (mg/L); "1 ppb" is equivalent to 1 microgram per liter.

	PM _{2.5}	PM ₁₀	SO ₂	NO ₂	CO	O ₃	Temp.
PM _{2.5}	1.000	0.583	0.181	0.561	0.677	-0.187	0.130
PM ₁₀	0.583	1.000	0.195	0.037	0.066	0.412	0.639
SO ₂	0.181	0.195	1.000	0.367	0.257	-0.075	0.231
NO ₂	0.561	0.037	0.367	1.000	0.952	-0.728	-0.400
CO	0.677	0.066	0.257	0.952	1.000	-0.716	-0.405
O ₃	-0.187	0.412	-0.075	-0.728	-0.716	1.000	0.670
Temp.	0.130	0.639	0.231	-0.400	-0.405	0.670	1.000

Table 2: Correlation matrix of the predictors (January 1, 2018 - December 17, 2022).

the $\mathcal{N}(0, 0.1)$ priors assume low, uncertain predictor effects centered around zero.

$$\beta \sim \mathcal{N}(\mathbf{0}, 0.1 * \mathbf{I})$$

where the covariate effects vector β follows a multivariate normal distribution; σ_{β} denotes the standard deviation for the multiplicative effect of the log-transformed additional covariate, and \mathbf{I} is the identity matrix. Covariate effects (β) follow a multivariate normal distribution for equal uncertainty across predictors, while uniform prior: Uniform(0,20), for σ_{AR} and σ_x allow wide exploration of variability.

3.4 Outcome model results and conclusions

This section contains the study findings with respect to the four targeted health outcomes. For each outcome, we provide the selected regression model results. Details about the model comparisons and significant predictors are provided in Table 5 in the Appendix. The results for the selected model of each specific outcome are plotted for each variable effect and included in the **Supplementary Material 4**.

3.4.1 Chronic obstructive pulmonary disease (COPD)

The analysis investigates predictors in relation to COPD. In the case of the full model, SO₂ comes out to be a robust positive predictor while temperature and PM₁₀ seem to have some protective effects. CO, NO₂, O₃, and PM_{2.5} have not shown clear associations in the study. Models for measurement error in each specific pollutant reveal that SO₂, temperature, and PM₁₀ are still significant effectors. The association with SO₂ is positive whereas those with temperature and PM₁₀ are protective. All measurement error models have lower WAIC values which indicate a slight improvement of fit.

A simpler model comprised solely of SO₂, temperature, and PM₁₀ is subjected to measurement error using log(SO₂) or log(PM₁₀). The model considering measurement error in log(SO₂) possesses the least WAIC, hence postulates to have the best fit. These relationships still hold true with temperature increasing by 1°C resulting in 1.3% reduction in COPD deaths (95% CI: 1.0% to 1.7%), increased SO₂ concentration of 10% resulting in 0.63% rise (95% CI: 0.28% to 0.99%) in COPD deaths, and lastly, a rise of 10% in PM₁₀ associated with decrease of death by 1.2% (95% CI: 0.67% to 1.7%).

When models include measurement error in one air pollutant, such as log(SO₂) or log(PM₁₀), alongside temperature, the direction of effects remains consistent. Temperature retains its negative association, while SO₂ and PM₁₀ maintain their positive and negative associations, respectively. However, these models exhibit slightly higher WAIC values.

3.4.2 Pneumonia

The analysis measures air pollutants in pneumonia and compares the predictions between complete models and simple models without or with measurement error. While full models indicated positive coefficients for pneumonia with CO and SO₂, temperature and PM₁₀ are negatively associated. NO₂ indicates an association with a negative direction, but such association is nonsignificant when measurement error is introduced into log(PM_{2.5}). Measurement error makes O₃ non-significant except when the introduction on measurement error in log(CO) occurs, in which case, it indicates a negative significant association. PM_{2.5} has no significant effect in all models. Simplifying these models by discarding PM_{2.5} confirms effects indicates in the models for CO, SO₂, temperature, and PM₁₀, but all yield WAIC higher than that of the complete model with measurement error on log(PM₁₀), in which each 1°C increase in temperature decreases pneumonia deaths by 1.7% (95% CI: 1.0% to 2.3%). A 10% increase in CO exposure is associated with 3.1% more pneumonia deaths (95% CI: 0.5% to 6.1%), whereas a 10% increase in NO₂ results in a 2.4% decrease (95% CI: 1.6% to 4.8%). SO₂ increases pneumonia deaths by 0.8% (95% CI: 0.3%-1.3%), whereas a 10% increase in PM₁₀ leads to a 1.5% decrease in pneumonia death (95% CI: 0.63%-2.4%).

3.4.3 Heart failure

The analysis evaluates the relationship between the predictors and heart failure outcomes. In the complete model, temperature is the only statistically significant predictor, while the others indicated credible intervals that included zero. When measurement error is introduced in either log(O₃) or log(PM_{2.5}), WAIC is reduced. This gives impetus towards further testing of the model. The final mixing of measurement error in log(O₃), temperature, and log(PM_{2.5}) gives the least WAIC indicating the best fit as well as predictive validity. For every decrease of 1°C of temperature heart failure deaths are reduced by 1.2% (95% credible interval: 0.7%-1.7%). A similar case occurs when O₃ exposure increases by 10% wherein there will be a corresponding drop in pneumonia deaths by 1.4%.

3.4.4 Malignant neoplasms

The analysis elaborates on the interplay among different predictors for malignant neoplasms. None of the predictors, including temperature, show a significant effect without measurement error, as credible intervals move through zero. Models considering measurement error also yield non-significant results, thus concluding that measurement error does not significantly affect conclusions. As indicated from the white-noise signal in the time series plot (Figure 4c), no predictor is expected to signal anything; the only-intercept model does not improve WAIC. However, when only considering temperature as a predictor, it shows that a 1°C increase leads to a decrease in Heart Failure death counts by 0.6% with a 95% credible interval of 0.3% - 0.9%. The temperature-only model has a lower WAIC than more complex models, demonstrating that adding other predictors does not significantly improve the explanatory power for counts of malignant neoplasm cases.

3.5 Temperature effect

Health Outcome	Estimate	95% Credible Interval	
		Lower Bound	Upper Bound
COPD	0.9820	0.9780	0.9850
Pneumonia	0.9740	0.9705	0.977
Heart Failure	0.9830	0.9790	0.9860
Malignant Neoplasm	0.9940	0.9905	0.9970

Table 3: Effect of temperature on health outcomes: An estimate of "a" indicates that for every 1°C increase in temperature, the expected death count is "a" times the original count.

Temperature consistently serves as a negative predictor as regards health, with increasing temperature translating into declining death counts for each condition, of self-protection. However, the strength of this relationship varies from condition to condition. Table 3 summarizes the temperature effects across health outcomes in temperature-only models. For every 1°C increase in temperature, death counts decrease by 1.8% for COPD, 2.6% for pneumonia (relative risk reduction 0.974), and 1.75% for heart failure due to less cardiovascular stress. Temperature plays a minor protective role (0.60% decrease in

cancer deaths per 1°C increase) for malignant neoplasm.

4 Discussion and Extension

In the MCMC algorithms, initialization of values and priors immensely contribute towards the convergence of a jags model due to the large parameter space. A good initialization is based on exploratory data analysis and prior knowledge of modeling performance. From the simulation studies, we see that both rjags and rstan are useful, but rjags comes first in terms of performance, with rstan serving as a validating tool. In scaling the original air pollution data, convergence is increasingly difficult because of multicollinearity (i.e CO is partially explained by NO₂), and extrapolated extreme values make the model more complicated. Log-transforming the predictors stabilizes variance and eliminates skewness, hence the value of this transformation to expedite convergence.

From our model results, we are aware of the fact that PM₁₀ has almost no effect on health outcomes, possibly indicating a protective effect. Meanwhile, PM_{2.5} prove to be insignificant. These findings could be attributed to low pollution levels, health impact thresholds, or external factors. This highlights the need for flexible models to account for unmeasured confounders. Temperature, however, is primarily associated with malignant neoplasm, aligning with the understanding that neoplasia is driven by long-term exposure rather than immediate environmental changes. Further studies are needed to explore whether this trend is specific to L.A. County and to understand whether it is influenced by the region, the model structure, or the data itself.

Our study is embedded with a measurement error only in one predictor, maintaining a balance between model accuracy and computational efficiency. Although increased robustness is achievable using advanced methods such as Bayesian hierarchical models or penalized regression, investigating measurement error in more predictors could yield results that are more realistic and comprehensive than this. Moving forward, the interaction between nasal and lung afflictions and viruses during the early stages of the COVID-19

pandemic warrants further investigation. Future studies could explore these interactions causally. The application of Geographic Information System (GIS) and spatiotemporal modeling will provide specific pollution patterns and high-risk areas, which would be integrated in the public health interventions.

Acknowledgement

This work received financial support from the Fonds de recherche du Québec (FRQ).

References

- [1] Michelle L Bell, Aidan McDermott, Scott L Zeger, Jonathan M Samet, and Francesca Dominici. Ozone and short-term mortality in 95 US urban communities, 1987-2000. *Journal of the American Medical Association*, 292(19):2372–2378, 2004.
- [2] Bert Brunekreef and Bertil Forsberg. Epidemiological evidence of effects of coarse airborne particles on health. *European Respiratory Journal*, 26(2):309–318, 2005.
- [3] Tze-Ming Chen, Ware G Kuschner, Janaki Gokhale, and Scott Shofer. Outdoor air pollution: nitrogen dioxide, sulfur dioxide, and carbon monoxide health effects. *The American Journal of the Medical Sciences*, 333(4):249–256, 2007.
- [4] Douglas W Dockery, C Arden Pope, Xiping Xu, John D Spengler, James H Ware, Martha E Fay, Benjamin G Ferris Jr, and Frank E Speizer. An Association between Air Pollution and Mortality in Six U.S. Cities. *New England Journal of Medicine*, 329(24):1753–1759, 1993.
- [5] Francesca Dominici, Roger D Peng, Michelle L Bell, Luu Pham, Aidan McDermott, Scott L Zeger, and Jonathan M Samet. Fine particulate air pollution and hospital admission for cardiovascular and respiratory diseases. *Journal of the American Medical Association*, 295(10):1127–1134, 2006.

- [6] Francesca Dominici, Scott L Zeger, and Jonathan M Samet. A measurement error model for time-series studies of air pollution and mortality. *Biostatistics*, 1(2):157–175, 2000.
- [7] Arlene M Fiore, Daniel J Jacob, Brendan D Field, David G Streets, Suneeta D Fernandes, and Carey Jang. Linking ozone pollution and climate change: The case for controlling methane. *Geophysical Research Letters*, 29(19):25–1–25–4, 2002.
- [8] Thomas J Grahame and Richard B Schlesinger. Cardiovascular health and particulate vehicular emissions: a critical evaluation of the evidence. *Air Quality, Atmosphere and Health*, 3:3–27, 2010.
- [9] Trevor Hastie and Robert Tibshirani. Generalized Additive Models: Some Applications. *Journal of the American Statistical Association*, 82(398):371–386, 1987.
- [10] Shui He, Sati Mazumdar, and Vincent C Arena. A comparative study of the use of GAM and GLM in air pollution research. *Environmetrics*, 17(1):81–93, 2006.
- [11] Ujjwal Kumar and VK Jain. ARIMA forecasting of ambient air pollutants (O₃, NO, NO₂ and CO). *Stochastic Environmental Research and Risk Assessment*, 24:751–760, 2010.
- [12] Duncan Lee and Gavin Shaddick. Modelling the effects of air pollution on health using Bayesian dynamic generalised linear models. *Environmetrics*, 19(8):785–804, 2008.
- [13] Dora Matzke, Alexander Ly, Ravi Selker, Wouter D Weeda, Benjamin Scheibehenne, Michael D Lee, and Eric-Jan Wagenmakers. Bayesian Inference for Correlations in the Presence of Measurement Error and Estimation Uncertainty. *Collabra: Psychology*, 3(1):25, 2017.
- [14] Donatella Pomata, Patrizia Di Filippo, Carmela Riccardi, Federica Castellani, Giulia Simonetti, Elisa Sonogo, and Francesca Buiarelli. Toxic Organic Contaminants in Airborne Particles: Levels, Potential Sources and Risk Assessment. *International Journal of Environmental Research and Public Health*, 18(8):4352, 2021.

- [15] Sylvia Richardson and Walter R Gilks. A Bayesian approach to measurement error problems in epidemiology using conditional independence models. *American Journal of Epidemiology*, 138(6):430–442, 1993.
- [16] Elmer Robinson. Some Air Pollution Aspects of the Los Angeles Temperature Inversion. *Bulletin of the American Meteorological Society*, 33(6):247–250, 1952.
- [17] Jonathan M Samet, Francesca Dominici, Frank C Curriero, Ivan Coursac, and Scott L Zeger. Fine Particulate Air Pollution and Mortality in 20 US Cities, 1987–1994. *New England Journal of Medicine*, 343(24):1742–1749, 2000.
- [18] Lianne Sheppard, Richard T Burnett, Adam A Szpiro, Sun-Young Kim, Michael Jerrett, C Arden Pope, and Bert Brunekreef. Confounding and exposure measurement error in air pollution epidemiology. *Air Quality, Atmosphere and Health*, 5:203–216, 2012.
- [19] Shengzhi Sun, Francine Laden, Jaime E Hart, Hong Qiu, Yan Wang, Chit Ming Wong, Ruby Siu-yin Lee, and Linwei Tian. Seasonal temperature variability and emergency hospital admissions for respiratory diseases: a population-based cohort study. *Thorax*, 73(10):951–958, 2018.
- [20] Joseph Sánchez-Balseca and Agustí Pérez-Foguet. Modelling hourly spatio-temporal PM_{2.5} concentration in wildfire scenarios using dynamic linear models. *Atmospheric Research*, 242:104999, 2020.
- [21] Kai-Chao Yao, Hsiu-Wen Hsueh, Ming-Hsiang Huang, and Tsung-Che Wu. The Role of GARCH Effect on the Prediction of Air Pollution. *Sustainability*, 14(8):4459, 2022.
- [22] Fengying Zhang, Liping Li, Thomas Krafft, Jinmei Lv, Wuyi Wang, and Desheng Pei. Study on the association between ambient air pollution and daily cardiovascular and respiratory mortality in an urban district of Beijing. *International Journal of Environmental Research and Public Health*, 8(6):2109–2123, 2011.
- [23] Xingyuan Zhou, Min Guo, Zhifei Li, Xiping Yu, Gang Huang, Zhen Li, Xiaohong Zhang, and Liya Liu. Associations between air pollutant and pneumonia and asthma

requiring hospitalization among children aged under 5 years in Ningbo, 2015–2017.
Front Public Health, 10:1017105, 2023.

Appendix

Scale	Pollutant	Estimates (dlm, jags, stan)	95% Credible Intervals (dlm, jags, stan)
Original	PM _{2.5}	$\phi = 0.991, 0.990, 0.99$ $\sigma_w^2 = 1.606, 2.026, 1.83$ $\sigma_v^2 = 8.216, 8.028, 8.51$	ϕ : [0.978 , 1.000], [0.975 , 0.999],[0.98, 1.00] σ_w^2 : [0.560 , 2.653], [1.007 , 3.574],[0.87, 3.33] σ_v^2 : [6.224 , 10.207], [6.191 , 9.742], [6.57, 10.76]
Log	PM _{2.5}	$\phi = 0.997, 0.997, 0.96$ $\sigma_w^2 = 0.013, 0.016, 0.21$ $\sigma_v^2 = 0.047, 0.047, 0.43$	ϕ : [0.991 , 1.000], [0.991, 0.9999], [0.93, 0.98] σ_w^2 : [0.005 , 0.022], [0.008, 0.028],[0.15, 0.28] σ_v^2 : [0.035 , 0.060], [0.034, 0.060],[0.34, 0.53]
Original	PM ₁₀	$\phi = 0.991, 0.989, 0.16$ $\sigma_w^2 = 10.21, 9.87, 1.34$ $\sigma_v^2 = 39.06, 9.93, 49.97$	ϕ : [0.978 , 1], [0.976 , 0.999], [0.03, 0.33] σ_w^2 : [4.524 , 15.905], [9.506 , 9.997], [1.07, 1.72] σ_v^2 : [29.542 , 48.580], [9.743 , 9.998], [49.91, 50.00]
Log	PM ₁₀	$\phi = 0.997, 0.997, 0.98$ $\sigma_w^2 = 0.026, 0.030, 0.20$ $\sigma_v^2 = 0.063, 0.062, 0.43$	ϕ : [0.992 , 1], [0.991 , 1.000], [0.96, 0.99] σ_w^2 : [0.012, 0.040], [0.017 , 0.050], [0.14, 0.27] σ_v^2 : [0.045 , 0.081], [0.044 , 0.081], [0.35, 0.54]
Original	CO	$\phi = 0.990, 0.991, 0.09$ $\sigma_w^2 = 0.002, 0.002, 0.01$ $\sigma_v^2 = 0.003, 0.003, 0.49$	ϕ : [0.979 , 1], [0.978 , 0.999], [0.01, 0.21] σ_w^2 : [0.001 , 0.002], [0.001 , 0.0037], [0, 0.02] σ_v^2 : [0.002 , 0.004], [0.002 , 0.004], [0.41, 0.58]
Log	CO	$\phi = 0.993, 0.993, 0.75$ $\sigma_w^2 = 0.011, 0.012, 0.36$ $\sigma_v^2 = 0.018, 0.018, 0.86$	ϕ : [0.984 , 1], [0.982 , 1.000], [0.67, 0.86] σ_w^2 : [0.007 , 0.016], [0.008 , 0.018], [0.26, 0.5] σ_v^2 : [0.013 , 0.023], [0.013 , 0.024], [0.69, 1.07]
Original	SO ₂	$\phi = 0.984, 0.984, 0.1$ $\sigma_w^2 = 0.003, 0.003, 0.01$ $\sigma_v^2 = 0.011, 0.011, 0.5$	ϕ : [0.968 , 1], [0.964 , 0.998], [0.01, 0.24] σ_w^2 : [0.001, 0.004], [0.002 , 0.005], [0, 0.02] σ_v^2 : [0.008, 0.014], [0.008, 0.014], [0.05, 0.6]
Log	SO ₂	$\phi = 0.990, 0.988, 0.78$ $\sigma_w^2 = 0.027, 0.033, 0.4$ $\sigma_v^2 = 0.134, 0.133, 0.98$	ϕ : [0.974 , 1], [0.969 , 0.999], [0.7, 0.85] σ_w^2 : [0.009 , 0.045], [0.016, 0.060], [0.26, 0.55] σ_v^2 : [0.101, 0.167], [0.101, 0.169], [0.78, 1.21]
Original	NO ₂	$\phi = 0.991, 0.991, 0.99$ $\sigma_w^2 = 2.229, 2.534, 3.19$ $\sigma_v^2 = 5.773, 5.742, 6.57$	ϕ : [0.9798297 , 1], [0.978 , 1.000], [0.98,1] σ_w^2 : [1.27, 3.18], [1.615, 3.846], [2.02, 4.79] σ_v^2 : [4.395, 7.152], [4.398, 7.306], [5.02, 8.43]
Log	NO ₂	$\phi = 0.998, 0.997, 0.96$ $\sigma_w^2 = 0.011, 0.013, 0.18$ $\sigma_v^2 = 0.026, 0.026, 0.38$	ϕ : [0.9933813 , 1], [0.993, 1.000], [0.94, 0.98] σ_w^2 : [0.007 , 0.016], [0.008 , 0.019], [0.13, 0.24] σ_v^2 : [0.020, 0.033], [0.020 , 0.033], [0.3, 0.47]
Original	O ₃	$\phi = 0.994, 0.994, 0.05$ $\sigma_w^2 = 7e - 6, 8e - 6, 0$ $\sigma_v^2 = 5e - 6, 6e - 6, 0.4$	ϕ : [0.986 , 1.000], [0.985 , 1.000], [0,0.13] σ_w^2 : [5e-06 , 10e-06], [5e-06 , 1e-05],[0, 0.01] σ_v^2 : [4e-06, 7e-06], [4e-06 , 8e-06], [0.32,0.45]
Log	O ₃	$\phi = 0.996, 0.998, 0.96$ $\sigma_w^2 = 0.010, 0.011, 0.76$ $\sigma_v^2 = 0.007, 0.007, 1.55$	ϕ : [0.999,1], [0.995,1.000], [0.93, 0.99] σ_w^2 : [0.007, 0.014], [0.008, 0.016], [0.55, 1.02] σ_v^2 : [0.004, 0.010], [0.004, 0.010], [1.25, 1.92]

Table 4: Parameter estimates of the AR process and measurement error for air pollution: comparison of the three Bayesian state-space model estimation approaches.

Note: " ϕ " represents the influence of past values of a time series on its current value; " σ_w^2 " is the AR1 process variance; " σ_v^2 " is the observation variance.

Outcome	Model Specification	WAIC	Significant Predictors	
COPD	all predictors on log scale w.o ⁵ ME ⁶	1824.8	SO ₂ + ⁷ , Temp ⁸⁻⁹ , PM ₁₀ -	
	all predictors on log scale w. ¹⁰ ME in log(CO)	1823.0	SO ₂ +, Temp-, PM ₁₀ -	
	all predictors on log scale w. ME in log(NO ₂)	1823.5	SO ₂ +, Temp-, PM ₁₀ -	
	all predictors on log scale w. ME in log(SO ₂)	1822.7	SO ₂ +, Temp-, PM ₁₀ -	
	all predictors on log scale w. ME in log(O ₃)	1815.5	SO ₂ +, Temp-, PM ₁₀ -	
	all predictors on log scale w. ME in log(PM _{2.5})	1821.8	SO ₂ +, Temp-, PM ₁₀ -	
	all predictors on log scale w. ME in log(PM ₁₀)	1817.7	SO ₂ +, Temp-, PM ₁₀ -	
	ME in log(SO ₂), Temp, log(PM ₁₀)	1813.3	SO ₂ +, Temp-, PM ₁₀ -	
	ME in log(PM ₁₀), Temp, log(SO ₂)	1814.9	SO ₂ +, Temp-, PM ₁₀ -	
	ME in log(SO ₂), Temp	1830.6	SO ₂ +, Temp-	
	ME in log(PM ₁₀), Temp	1824.2	Temp-, PM ₁₀ -	
	Temp	1840.0	Temp-	
	Pneumonia	all predictors on log scale w.o ME	1779.3	CO+, SO ₂ +, Temp-, NO ₂ -, PM ₁₀ -
		all predictors on log scale w. ME in log(CO)	1771.8	CO+, SO ₂ +, Temp-, NO ₂ -, O ₃ -, PM ₁₀ -
all predictors on log scale w. ME in log(NO ₂)		1771.1	CO+, SO ₂ +, Temp-, NO ₂ -, PM ₁₀ -	
all predictors on log scale w. ME in log(SO ₂)		1772.6	CO+, SO ₂ +, Temp-, NO ₂ -, PM ₁₀ -	
all predictors on log scale w. ME in log(O ₃)		1773.7	CO+, SO ₂ +, Temp-, NO ₂ -, PM ₁₀ -	
all predictors on log scale w. ME in log(PM _{2.5})		1771.1	CO+, SO ₂ +, Temp-, PM ₁₀ -	
all predictors on log scale w. ME in log(PM ₁₀)		1770.6	CO+, SO ₂ +, Temp-, NO ₂ -, PM ₁₀ -	
ME in log(CO), log(NO ₂), Temp, log(SO ₂), log(O ₃), log(PM ₁₀)		1775.8	CO+, SO ₂ +, Temp-, PM ₁₀ -	
ME in log(NO ₂), log(CO), Temp, log(SO ₂), log(O ₃), log(PM ₁₀)		1773.8	CO+, SO ₂ +, Temp-, PM ₁₀ -	
ME in log(SO ₂), Temp, log(CO), log(NO ₂), log(O ₃), log(PM ₁₀)		1773.3	CO+, SO ₂ +, Temp-, PM ₁₀ -	
ME in log(O ₃), Temp, log(CO), log(NO ₂), log(SO ₂), log(PM ₁₀)		1774.1	CO+, SO ₂ +, Temp-, PM ₁₀ -	
ME in log(PM ₁₀), Temp, log(CO), log(NO ₂), log(SO ₂), log(O ₃)		1775.5	CO+, SO ₂ +, Temp-, PM ₁₀ -	
ME in log(CO), Temp		1785.5	CO+, Temp-	
ME in log(NO ₂), Temp		1792.7	NO ₂ -, Temp-	
ME in log(SO ₂), Temp		1791.6	SO ₂ +, Temp-	
ME in log(PM ₁₀), Temp		1809.7	Temp-	
ME in log(O ₃), Temp		1787.2	Temp-	
Temp		1812.0	Temp-	
Heart Failure		all predictors on log scale w.o ME	1790.1	Temp-
		all predictors on log scale w. ME in log(CO)	1768.6	Temp-
	all predictors on log scale w. ME in log(NO ₂)	1768.6	Temp-	
	all predictors on log scale w. ME in log(SO ₂)	1767.7	Temp-	
	all predictors on log scale w. ME in log(O ₃)	1764.6	Temp-	
	all predictors on log scale w. ME in log(PM _{2.5})	1764.8	Temp-	
	all predictors on log scale w. ME in log(PM ₁₀)	1768.5	Temp-	
	ME in log(O ₃), Temp	1761.9	Temp-	
	ME in log(PM _{2.5}), Temp	1762.0	Temp-	
	ME in log(O ₃), Temp, log(PM _{2.5})	1756.9	Temp-, O ₃ -	
	ME in log(PM _{2.5}), Temp, log(O ₃)	1782.1	Temp-, O ₃ -	
	Temp	1767.3	Temp-	
	Malignant Neoplasms	all predictors on log scale no ME	1759.8	/
all predictors on log scale w. ME in log(CO)		1721.3	/	
all predictors on log scale w. ME in log(NO ₂)		1716.6	/	
all predictors on log scale w. ME in log(SO ₂)		1726.8	/	
all predictors on log scale w. ME in log(O ₃)		1719.2	/	
all predictors on log scale w. ME in log(PM _{2.5})		1719.0	/	
all predictors on log scale w. ME in log(PM ₁₀)		1723.9	/	
Temp		1716.3	Temp-	
intercept		1730.4	-	

Table 5: Model specifications and WAIC comparisons.

Note: "w.o." = without; "ME" = measurement error; "w." = with; "Temp" = temperature; "+" indicates the predictor has a significant positive effect in the specified model; "-" indicates the predictor has a significant negative effect in the specified model.

Supplementary Material

Analysis Methodology

A total of 11 air quality monitoring stations accredited by the [U.S. Environmental Protection Agency \(EPA\)](#) have been established in Los Angeles County, California, USA. These 11 stations collect daily particulate matter measurements (PM_{2.5} and PM₁₀), nitrogen dioxide (NO₂), carbon monoxide (CO), sulfur dioxide (SO₂), and ozone (O₃) from their site. The data are submitted by stations daily, every three days, or every six days,

and sometimes reported gaps occur due to malfunctions or other reporting issues. Averages for each day and week which have been used to construct consistent time series using aggregation methods have been calculated alongside the MMWR (Morbidity and Mortality Weekly Report) weeks¹¹ specific to this study.

For each air pollutant, on each day (d), the daily measure (p_d) is computed by averaging all available observations of the specific air pollutant collected across the monitoring stations on that day. If $p_{d,1}, p_{d,2}, \dots, p_{d,n}$ represent the n valid measurements available for day d , the daily average is calculated by:

$$p_d = \frac{1}{n} \sum_{i=1}^n p_{d,i}, \text{ with } i \in \{1, 2, \dots, n\}$$

where n is the number of valid observations of the specified air pollutant on the day d .

The weekly average P_t is the mean of the daily measures from the same MMWR week:

$$P_t = \frac{1}{m_t} \sum_{j \in J_t} p_j$$

where J_t is the set of valid day indices in week t , with $J_1 = \{2, 3, 4, 5, 6, 7\}$ and $J_t = \{1, 2, 3, 4, 5, 6, 7\}$ for all the other weeks. p_j represents the daily measurement for a day $j \in J_t$, and m_t is the number of valid days of week t , with $m_1 = 6$ and $m_t = 7$ for the other weeks. This method refers to as 7-day average smooths day-to-day variations but does not remove the error in measurement in the P_t produced.

The daily temperature means for L.A. County are sourced from [NOAA's NClmGrid Daily Averages](#). MMWR weekly mean temperatures are calculated by averaging the corresponding MMWR daily means.

The population data for L.A. County (Figure 5 in Appendix) comes from the [Federal Reserve Economic Data \(FRED\)](#) platform, specifically the series [CALOSA7POP](#), which provides annual population estimates from 1970 onward. Weekly population values are

¹¹MMWR weeks are the periods from Sunday to Saturday, which can fall within range 1 to 52.

estimated via linear regression, assuming a relationship between year (t) and population (Y_t):

$$Y_t = \beta_0 + \beta_1 t + \epsilon_t, \quad \epsilon_t \sim \mathcal{N}(0, \sigma^2)$$

where β_0 is the intercept, β_1 is the slope, and ϵ_t is a normally distributed error term.

The CDC WONDER platform allows reporting the availability of health-related datasets, including weekly county-level counts of respiratory and cardiovascular deaths, along with some quality and temperature data from January 1, 2018, to December 17, 2022. These data are available through the [About Provisional Mortality Statistics, 2018 through Last Week](#), and the source is the [Centers for Disease Control and Prevention \(CDC\)](#), which consists of death certificate records with underlying and additional causes as well as demographic information and category breakdowns. Respiratory deaths by ICD-10 codes ¹²are defined by the range: J00-J98. Correspondingly cardiovascular deaths are defined by ICD-10 code I50.0 (heart failure). The data, however, are provisional and counted less than ten is suppressed for confidentiality, while over ten counts have undergone amendments pending the processing of certificates for more records. Weekly counts for each health outcome exceed 15 throughout the study period, resulting in no missing values in the extracted dataset.

Simulation Study

State space model simulation studies

A state space model is applied to capture both the temporal dependencies within the time series and the observation noise of the measurements:

1. **State Equation:** The true pollutant concentration X_t evolves over time as:

$$X_t = \phi X_{t-1} + w_t, \quad w_t \sim \text{Normal}(0, \sigma_w^2), \quad (3)$$

¹²ICD10 is the 10th Revision of the International Classification of Diseases (ICD), a medical classification list by the World Health Organization (WHO).

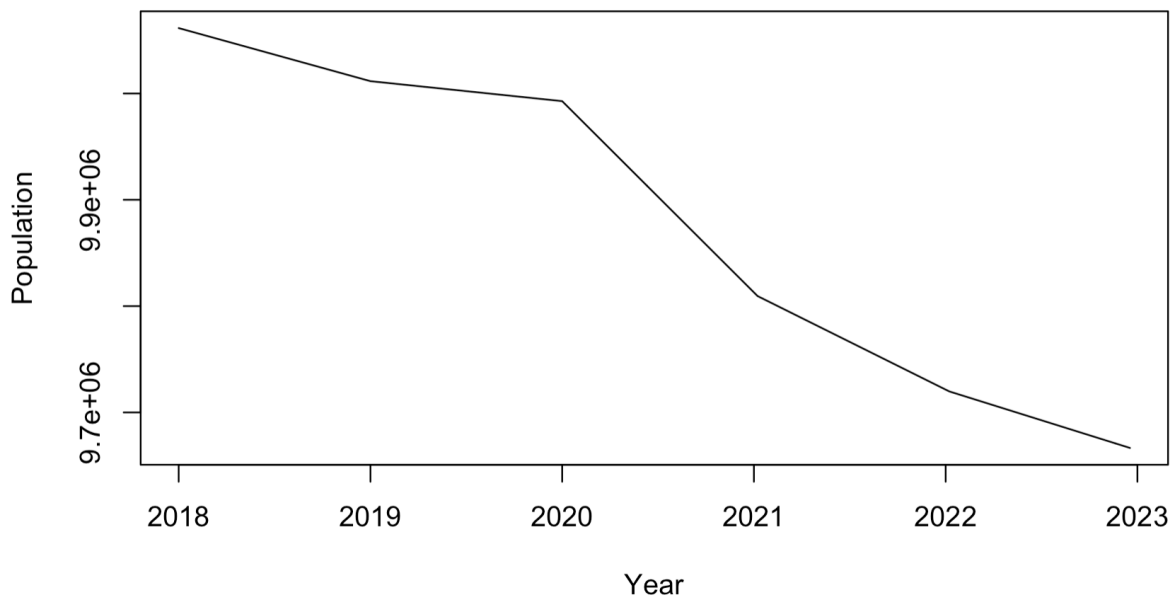


Figure 5: Population size time series in L.A. county (January 1, 2018 - December 17, 2022)

where ϕ is the autoregressive parameter, and σ_w^2 is the process noise variance.

- 2. Observation Equation:** The observed concentration Y_t is related to the true exposure X_t through an observation equation that incorporates measurement error:

$$Y_t = X_t + v_t, \quad v_t \sim \text{Normal}(0, \sigma_v^2), \quad (4)$$

where σ_v^2 denotes the variance of the observation noise.

Simulation studies are done with the `d1m`, `rjags`, and `rstan` packages that show distinct approaches to parameter estimation in state-space models. For Y_t simulated with $\mu_x = 10$, $\phi = 0.7$, $\sigma_w^2 = 0.5$, and $\sigma_v^2 = 0.9$, `d1m` estimates $\phi = 0.79$ (95% Confidence Interval: [0.73, 0.86]), $\sigma_w^2 = 0.18$ (95% Confidence Interval: [0, 0.37]), and $\sigma_v^2 = 1.03$ (95% Confidence Interval: [0.63, 1.42]). In `rjags`, the same model gives $\phi = 0.7456$ with 95% Credible Interval(CI) being [0.6185, 0.8486]), $\sigma_w^2 = 0.5404$ (95% CI [0.2069, 1.1535]), and $\sigma_v^2 = 0.6840$ (95% CI [0.2542, 1.1321]). Using `rstan`, estimates are $\phi = 0.70$ (95% CI [0.59, 0.79]), $\sigma_w^2 = 0.30$ (95% CI [0.07, 0.72]), and $\sigma_v^2 = 1.01$ (95% CI [0.61, 1.50]). A summary is shown in Table 6.

Method	Parameter	True Value	Estimate	95% CI
d1m	ϕ	0.7	0.79	[0.73, 0.86]
	σ_w^2	0.5	0.18	[0.00, 0.37]
	σ_v^2	0.9	1.03	[0.63, 1.42]
rjags	ϕ	0.7	0.7456	[0.6185, 0.8486]
	σ_w^2	0.5	0.5404	[0.2069, 1.1535]
	σ_v^2	0.9	0.6840	[0.2542, 1.1321]
rstan	ϕ	0.7	0.70	[0.59, 0.79]
	σ_w^2	0.5	0.30	[0.07, 0.72]
	σ_v^2	0.9	1.01	[0.61, 1.50]

Table 6: State Space Model Results for Different Methods.

Outcome model simulation studies

To evaluate whether the model would work in our real data analysis, we simulate the outcome data Y_t in a manner that mimics the real situation:

$$Y_t \sim \text{Poisson}(\lambda_t), \quad (5)$$

where

$$\log(\lambda_t) = \beta_0 + \beta_1 X_{\text{true},t} + \beta_2 X_{2,t} + \beta_3 X_{3,t} + \log(\text{offset},t), \quad (6)$$

Measurement error is introduced into the observed predictor variable X , such that:

$$X_{\text{obs},t} = X_{\text{true},t} + \delta/n_t, \quad (7)$$

where $\delta \sim \text{Normal}(0, \sigma_x^2)$ represents the measurement error and n represents a vector of fixed constant.

If Y is generated under the model (Equations (5), (6), (7)) with $\beta_0 = 10$, $\beta_1 = -1$, $\beta_2 = 0$, $\beta_3 = 0$, and $\delta = 0$ (i.e measurement errors do not exist in X), the model fitting using rjags gives $\beta_0 = 9.92$ (95% CI: 9.83–10.01) and $\beta_1 = -0.99$ (95% CI: -1.00 to -0.97) with a WAIC of 1144.7, excellent convergence, and a sufficiently large effective sample size. In the absence of measurement error, the output of rstan is $\beta_0 = 9.99$ (95% CI: [9.90, 10.08]) and $\beta_1 = -1$ (95% CI: [-1.02, -0.99]) with a WAIC of 1093.8. Including measurement

error in the predictors distorts the parameter estimated by rjags, leading to divergence and a WAIC of 1207.5. Running the same model in rstan, the WAIC rises to 1154.8; the parameter estimates are distorted and the algorithm shows a divergence and small effective sample sizes even after 52,000 iterations. Table 7 is provided as a summary. To

Method	Fitting Measurement Error in X	β_0 [95% CI]	β_1 [95% CI]	WAIC
rjags	No	9.92 [9.83, 10.01]	-0.99 [-1.00, -0.97]	1144.7
rstan	No	9.99 [9.90, 10.08]	-1.00 [-1.02, -0.99]	1093.8
rjags	Yes	Distorted	Distorted	1207.5
rstan	Yes	Distorted	Distorted	1154.8

Table 7: Results of Simulated Outcome Model Fitting with and without Measurement Error when Y is generated without considering any measurement error in the predictor X.

explore how the fitted models would perform when Y is simulated from predictors: X_{obs} with measurement error, X_1 and X_2 based on the above setting, we simulate the outcome data Y_t with $\beta_0 = 10$, $\beta_1 = -1$, $\beta_2 = 0.1$, $\beta_3 = -0.5$, $\phi = 0.5$, $\sigma_{AR} = 2$, $\sigma_x = 4$. The true predictor (X_{true}) are generated using an AR(1) process:

$$X_{true,t} = \phi x_{true,t-1} + \epsilon_t, \quad \epsilon_t \sim \mathcal{N}. \quad (8)$$

When including measurement error in X_{obs} and accounting for the AR(1) nature of the data, as the structure shown in Equation 8, the fitted model with all three predictors returns the following rjags estimates: $\beta_0 = 9.04$ (95% CI: [8.29, 9.88]), $\beta_1 = -0.90$ (95% CI: [-0.99, -0.82]), $\beta_2 = 0.08$ (95% CI: [0.03, 0.13]), $\beta_3 = -0.48$ (95% CI: [-0.55, -0.41]), $\phi = 0.41$ (95% CI: [0.29, 0.52]), $\sigma_{AR} = 2.12$ (95% CI: [1.88, 2.39]), and $\sigma_x = 3.90$ (95% CI: [3.56, 4.27]), with a WAIC of 1780.1. When the same model is implemented using rstan, the estimates are: $\beta_0 = 0.91$ (95% CI: [0.73, 1.11]), $\beta_1 = -0.31$ (CI: [-0.35, -0.27]), $\beta_2 = 0.13$ (CI: [0.08, 0.18]), $\beta_3 = -0.45$ (CI: [-0.53, -0.38]), $\phi = 0.69$ (CI: [0.58, 0.78]), $\sigma_{AR} = 7.08$ (CI: [6.74, 8.05]), and $\sigma_x = 21.07$ (CI: [18.95, 23.66]), with a WAIC of 1804.8. Here, the estimates often fall outside the CIs, despite posterior convergence; the summary table 8 is shown as below.

Method	Parameter	True value	Estimate	95% CI	WAIC
rjags	β_0	10	9.04	[8.29, 9.88]	1780.1
	β_1	-1	-0.90	[-0.99, -0.82]	
	β_2	0.1	0.08	[0.03, 0.13]	
	β_3	-0.5	-0.48	[-0.55, -0.41]	
	ϕ	0.5	0.41	[0.29, 0.52]	
	σ_{AR}	2	2.12	[1.88, 2.39]	
	σ_x	4	3.90	[3.56, 4.27]	
rstan	β_0	10	0.91	[0.73, 1.11]	1804.8
	β_1	-1	-0.31	[-0.35, -0.27]	
	β_2	0.1	0.13	[0.08, 0.18]	
	β_3	-0.5	-0.45	[-0.53, -0.38]	
	ϕ	0.5	0.69	[0.58, 0.78]	
	σ_{AR}	2	7.08	[6.74, 8.05]	
	σ_x	4	21.07	[18.95, 23.66]	

Table 8: Results of Simulated Outcome Model Fitting Using Observed Predictors with Measurement Error. Models were fitted with rjags and rstan under the settings described in the text. While both methods achieve posterior convergence, rstan exhibits estimates outside the 95% credible intervals in some cases, indicating potential modeling challenges.

When fitting the model with X_{obs} on its log-scale (Table tab:logscale-results), the rjags estimates change: $\beta_0 = 12.98$ (95% CI: [11.86, 15.76]), $\beta_1 = -5.77$ (95% CI: [-8.06, -5.24]), $\beta_2 = 0.13$ (95% CI: [0.01, 0.88]), $\beta_3 = -0.58$ (95% CI: [-1.70, -0.40]), $\phi = 0.99$ (95% CI: [0.98, 1]), $\sigma_{\text{AR}} = 0.66$ (95% CI: [0.57, 0.85]), and $\sigma_x = 0.63$ (95% CI: [0.50, 1.24]), with a WAIC of 1801.3. If the model is implemented using rstan, the parameter estimates change as follows: $\beta_0 = 0.72$ (95% CI: [0.52, 0.89]), $\beta_1 = -0.98$ (95% CI: [-1.06, -0.9]), $\beta_2 = 0.09$ (95% CI: [0.04, 0.15]), $\beta_3 = -0.46$ (95% CI: [-0.54, -0.37]), $\phi = 0.97$ (95% CI: [0.94, 1]), $\sigma_{\text{AR}} = 2.35$ (95% CI: [2.08, 2.62]), and $\sigma_x = 6.04$ (95% CI: [5.48, 6.67]), with a WAIC of 1816.9. The increase in WAIC indicates a worse model fit due to the incorrect data scaling.

Using only X_{obs} as a predictor with measurement error leads to divergence and a WAIC of 2353.1 in rjags. For the same model implemented using rstan, the estimates are: $\beta_0 = 0.64$ (95% CI: [0.44, 0.84]), $\beta_1 = -1.03$ (95% CI: [-1.14, -0.93]), $\phi = 0.96$ (95% CI: [0.93, 0.99]), $\sigma_{\text{AR}} = 2.72$ (95% CI: [2.4, 3.04]), and $\sigma_x = 6.66$ (95% CI: [5.89, 7.42]), with a WAIC of 1819.6, indicating a worse fit than fitting with the full set of predictors (Table

Method	Parameter	True Value	Estimate	95% CI	WAIC
rjags	β_0	10	12.98	[11.86, 15.76]	1801.3
	β_1	-1	-5.77	[-8.06, -5.24]	
	β_2	0.1	0.13	[0.01, 0.88]	
	β_3	-0.5	-0.58	[-1.70, -0.40]	
	ϕ	0.5	0.99	[0.98, 1]	
	σ_{AR}	2	0.66	[0.57, 0.85]	
	σ_x	4	0.63	[0.50, 1.24]	
rstan	β_0	10	0.72	[0.52, 0.89]	1816.9
	β_1	-1	-0.98	[-1.06, -0.9]	
	β_2	0.1	0.09	[0.04, 0.15]	
	β_3	-0.5	-0.46	[-0.54, -0.37]	
	ϕ	0.5	0.97	[0.94, 1]	
	σ_{AR}	2	2.35	[2.08, 2.62]	
	σ_x	4	6.04	[5.48, 6.67]	

Table 9: Results of Simulated Outcome Model Fitting with Log-Scaled Predictors. The increase in WAIC for both **rjags** and **rstan** indicates a worse model fit due to the incorrect scaling of data. Despite posterior convergence, parameter estimates vary significantly.

10).

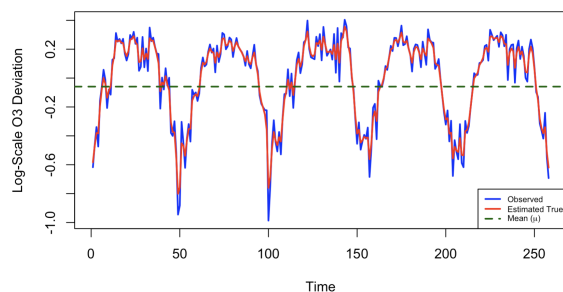
Method	Parameter	Estimate	95% CI	WAIC
rjags	Divergence	-	-	2353.1
rstan	β_0	0.64	[0.44, 0.84]	1819.6
	β_1	-1.03	[-1.14, -0.93]	
	ϕ	0.96	[0.93, 0.99]	
	σ_{AR}	2.72	[2.4, 3.04]	
	σ_x	6.66	[5.89, 7.42]	

Table 10: Results of Simulated Outcome Model Fitting Using Only X_{obs} as a Predictor with Measurement Error. Using **rjags** results in divergence and a high WAIC, while **rstan** provides stable parameter estimates but indicates a worse model fit compared to fitting the full set of predictors.

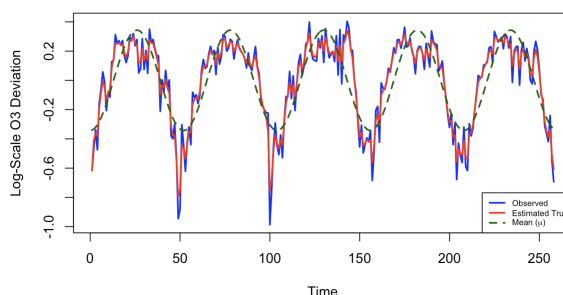
WAIC effectively indicates measurement error in predictors, with lower WAIC when error is included in models where it exists, and better performance without it otherwise. Full sets of properly scaled predictors and measurement error improve fit, precision and predictive accuracy. Besides the more robust convergence without explicit initial values, **rjags** also provides better estimates closer to true values than those produced by **rstan**, making **rjags** a clear winner as the preferred tool for state-space models and AR(1)

processes.

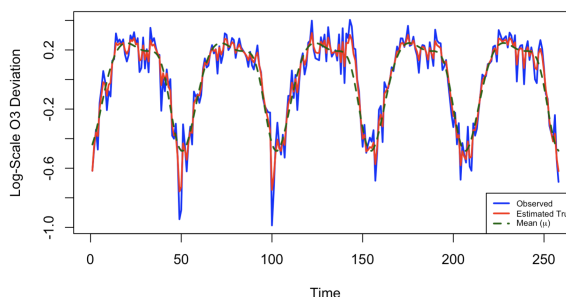
Application to the Los Angeles County Data



(a) Time-invariant model



(b) Time-varying model 1



(c) Time-varying model 2

Figure 6: Plots of Log-Scale Deviations in O_3 Concentrations: Real vs. Estimated Real Values and Estimated Mean.

The observed log-scaled predictors and their estimated true values on the log scale (Figure 7), from the AR(1) time-invariant-mean model, are reasonably similar, indicating that the Dynamic Linear Model (DLM) effectively captures the underlying relationships between the predictors and their true values. This alignment of observed and estimated values indicates that the model's state estimation process works well, and it has the minimum difference between the scaled predictors and their corresponding true values. Also,

the observed measure provides evidence of the noise taken into consideration with measurement error under a reasonable environment for estimating the true underlying values of the predictors. From a temporal standpoint, it is an appropriate model for capturing short-term dependencies within the data on the basis of an AR(1) model, given that one can expect a current value to be influenced by the immediately previous value. The invariant-mean-AR(1)-model offers a sound base for true value estimation from log-scaled predictors while at the same time accounting for short-term time dependencies.

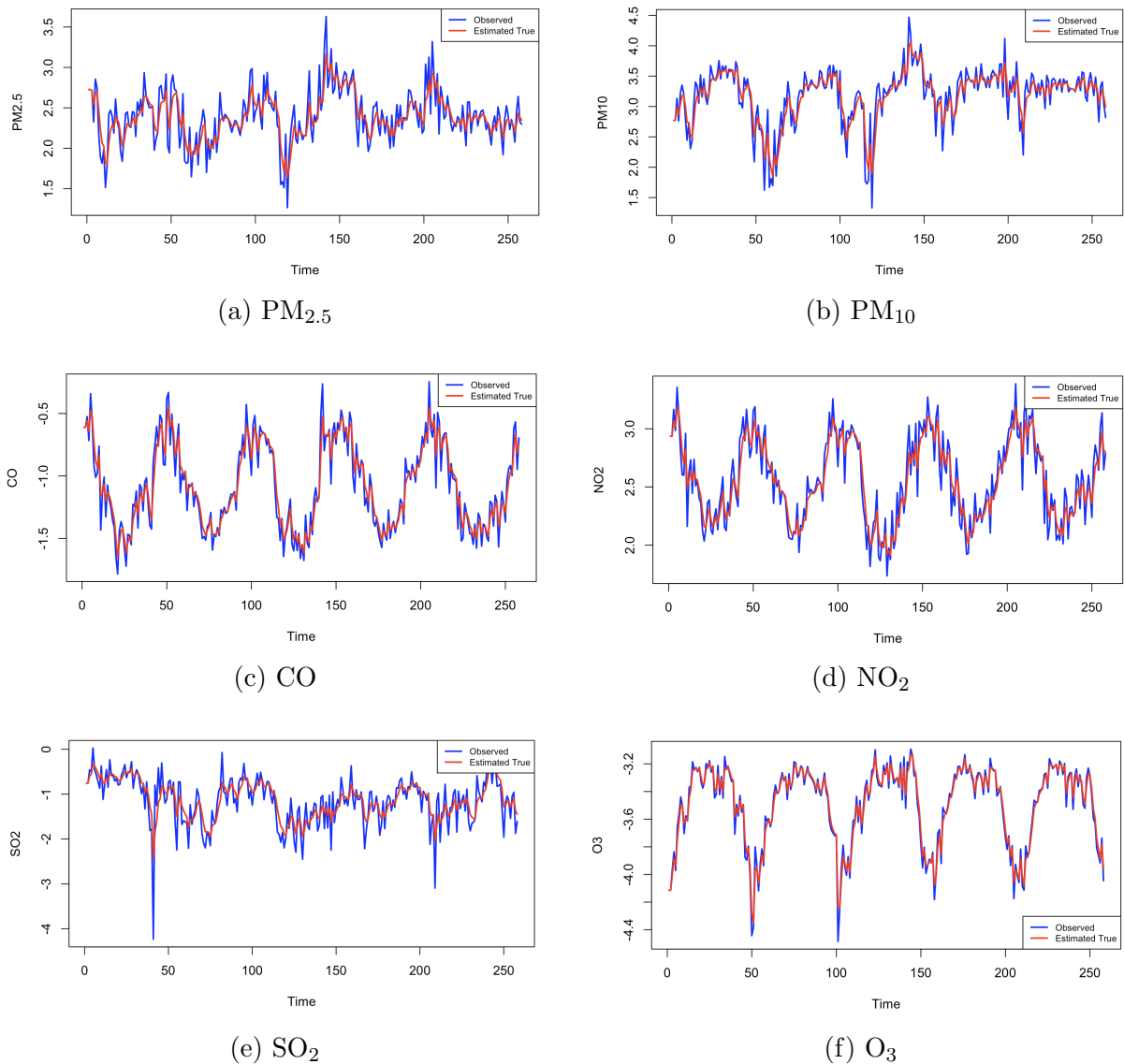


Figure 7: Time series of log-scaled observed and true exposure levels from the state space model for various pollutants.

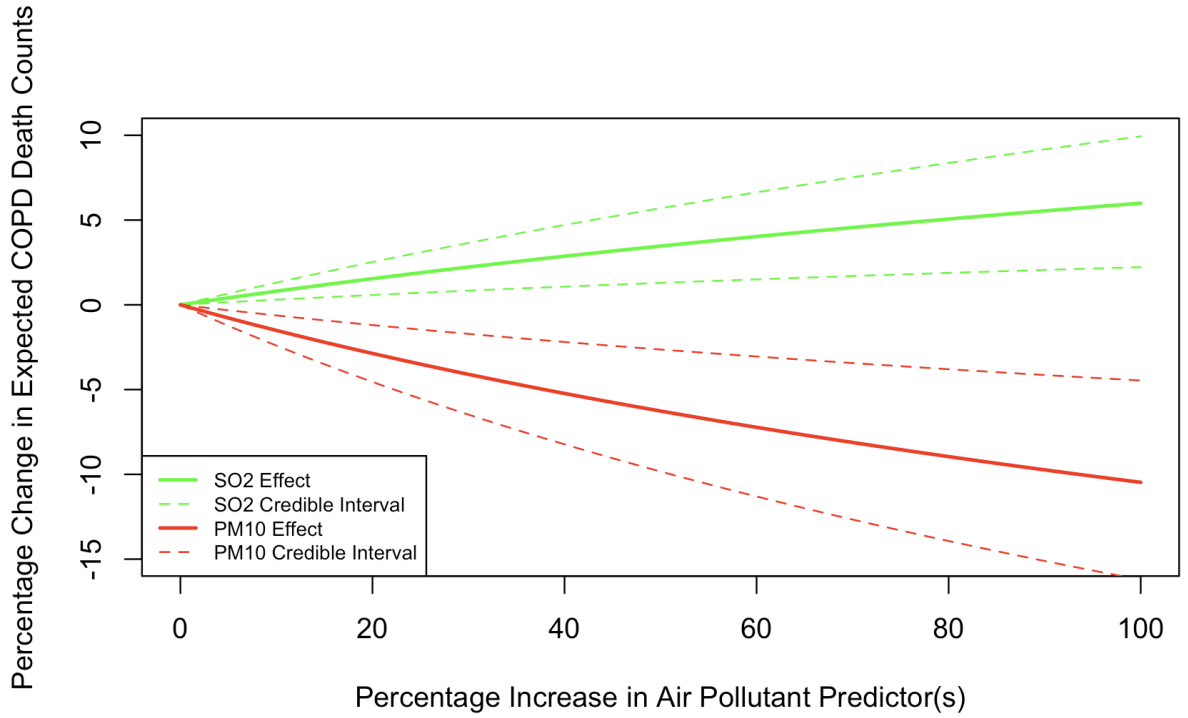


Figure 8: Percentage change in COPD deaths due to lag-1 SO_2 or PM_{10} change, holding other variables constant, Los Angeles County (Jan 8, 2018–Dec 17, 2022).

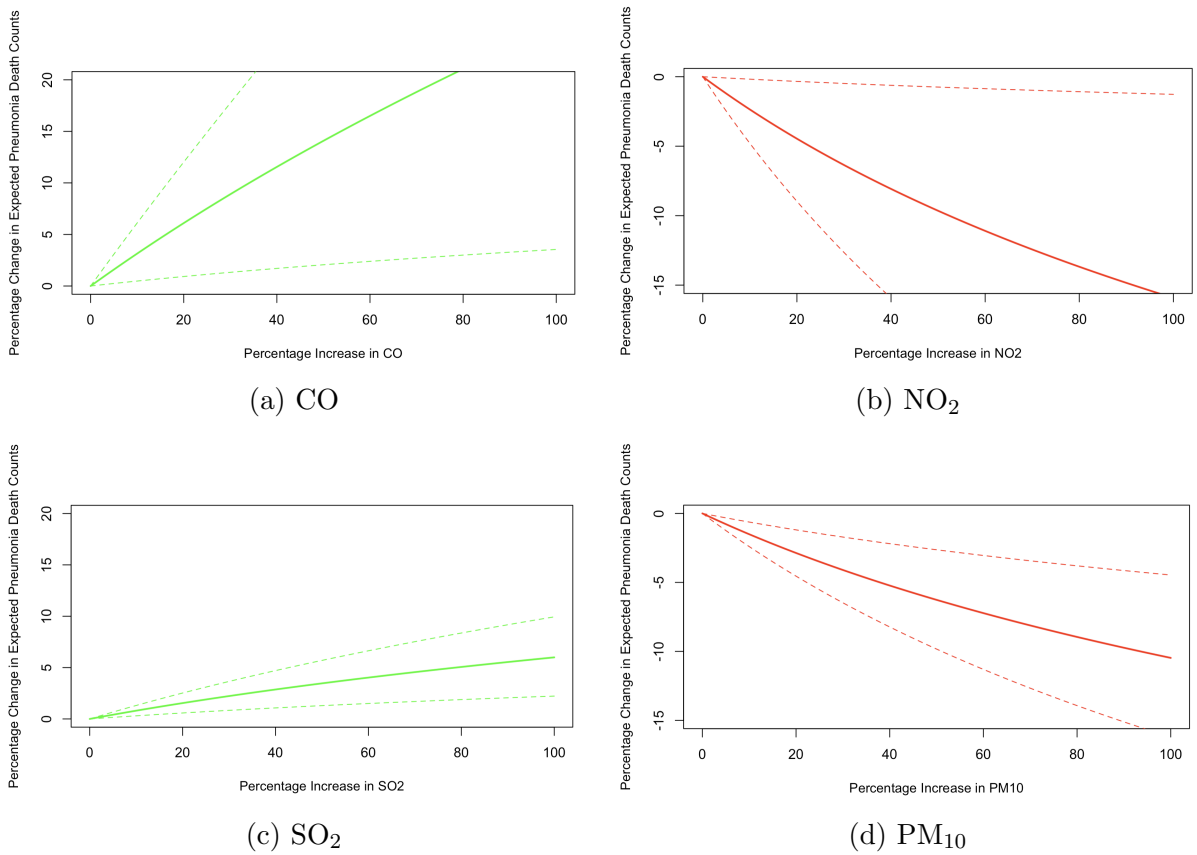


Figure 9: Percentage change in Pneumonia deaths due to lag-1 air pollutant changes in Los Angeles County (Jan 8, 2018–Dec 17, 2022).

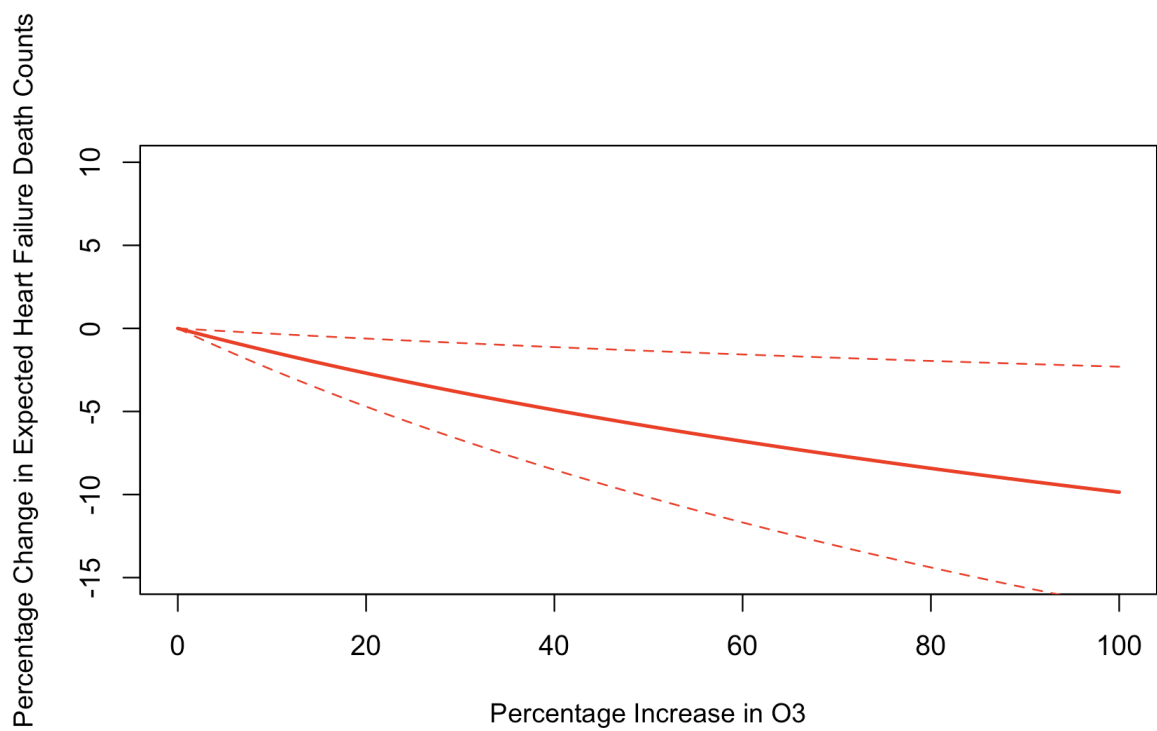


Figure 10: Percentage change in expected Heart failure deaths due to lag-1 O_3 change, holding other variables constant, in Los Angeles County (Jan 8, 2018–Dec 17, 2022).